surrounded by irrotational fluid, the two circuits C_1 and C_2 drawn in Fig. 4 enclose the same vortex tube, such that the first Helmholtz vortex law requires the circulation about these two circuits to be the same. Defining a variable ξ that measures distance along the vortex loop and has the value zero at the vortex loop tip, the strength $\Gamma_S(\xi, t)$ of the vortex loop at a location ξ is related to the strength $\gamma(\xi, t)$ of the vortex sheet spanning the region in between the loop legs by

$$\Gamma_S(\xi, t) = \int_0^{\xi} \gamma(\xi', t)\, \mathrm{d}\xi' + \Gamma_0 \tag{2}$$

where Γ_0 is the vortex strength at the loop tip. To simplify the problem, we assume that the vortex sheet strength has a constant value γ_0 at the point where it is shed from the cylinder and that the vortex sheet is ejected outward from the cylinder face at a constant speed V_E. This assumption is supported by the computational results of Ref. 9, which cover the time period during which the ejected vorticity wraps approximately one time around the primary vortex. The result [Eq. (2)] indicates that the vortex loop strength varies linearly both with time at a fixed cross section and with distance along the loop at a fixed time with slopes given by $(\partial\Gamma_S/\partial\xi)|_t = \gamma_0$ and $(\partial\Gamma_S/\partial t)|_{\xi_B - \xi} = \gamma_0 V_E$, where ξ_B is the value of ξ at the point where the vortex loop attaches to the cylinder. These slopes are compared to computational data of Ref. 9 for a case in which the vortex is inserted impulsively in a flow with no freestream velocity and $S/D = 0.3$. In the Ref. 9 computations the ejection velocity of the vortex sheet from the cylinder face is observed to maintain a nearly constant value $V_E \cong 0.44\,\Gamma/D$, which is comparable to, but slightly larger than, the velocity $0.38\Gamma/D$ induced by the columnar vortex (in isolation) evaluated at the ejection point. Estimating γ_0 using the correlation for the inviscid slip velocity W at the separation point gives $\gamma_0 \cong \max(-W) = 0.22\,\Gamma/S$. Lines having the theoretically predicted slopes for this case are shown in Fig. 5 to agree well with the computational data, which cover moderately short times after vorticity ejection from the cylinder. Over long times, it is likely that the increase in loop strength is limited by detachment and shedding of the loop from the cylinder surface.

V. Conclusions

Analytical models are presented for aspects of the flow observed during normal interaction of a columnar vortex and a circular cylinder, including onset of outward ejection of secondary vorticity from the cylinder boundary layer and variation of the strength of the ensuing vortex loop as a function of time and position along the loop. It is found that vorticity is ejected from the boundary layer along the cylinder leading edge when the vortex-cylinder separation distance decreases below a critical value, which varies approximately in proportion to the ratio of vortex strength to normal freestream velocity. Once vorticity is ejected from the cylinder boundary layer, it forms a looplike shape that wraps around the columnar vortex. Another model is introduced for the spatial and temporal variation of the strength of the ejected vortex loop, which is controlled by roll-up of the vortex sheet that is continually ejected from the cylinder boundary layer. Both the model for vorticity ejection onset and that for variation of vortex loop strength are found to be in excellent agreement with previous experimental and computational data. Although the current Note focuses on vortex interaction with a circular cylinder because data on the secondary vorticity field are available for this case, the models presented in the Note also apply to vortex interaction with elongated bodies of other cross-sectional shapes, such as helicopter rotor or marine propeller blades and control surfaces.

Acknowledgments

Research support was provided by the U.S. Army Research Office under Grant DAAH04-96-1-0081 with the University of Iowa. Thomas L. Doligalski is the Program Manager.

References

[1]Rockwell, D., "Vortex-Body Interactions," *Annual Review of Fluid Mechanics*, Vol. 30, 1998, pp. 199–229.

[2]Affes, H., and Conlisk, A. T., "Model for Rotor Tip Vortex-Airframe Interaction. Part 1: Theory," *AIAA Journal*, Vol. 31, No. 12, 1993, pp. 2263–2273.

[3]Marshall, J. S., and Yalamanchili, R., "Vortex Cutting by a Blade. Part II: Computations of Vortex Response," *AIAA Journal*, Vol. 32, No. 7, 1994, pp. 1428–1436.

[4]Kim, J. M., and Komerath, N. M., "Summary of the Interaction of a Rotor Wake with a Circular Cylinder," *AIAA Journal*, Vol. 33, No. 3, 1995, pp. 470–478.

[5]Doligalski, T. L., Smith, C. R., and Walker, J. D. A., "Vortex Interaction with Walls," *Annual Review of Fluid Mechanics*, Vol. 26, 1994, pp. 573–616.

[6]Affes, H., Xiao, Z., and Conlisk, A. T., "The Boundary-Layer Flow Due to a Vortex Approaching a Cylinder," *Journal of Fluid Mechanics*, Vol. 275, 1994, pp. 33–57.

[7]Xiao, Z., Burggraf, O. R., and Conlisk, A. T., "The Interacting Boundary-Layer Flow Due to a Vortex Approaching a Cylinder," *Journal of Fluid Mechanics*, Vol. 346, 1997, pp. 319–343.

[8]Krishnamoorthy, S., Gossler, A. A., and Marshall, J. S., "Normal Vortex Interaction with a Circular Cylinder," *AIAA Journal*, Vol. 37, No. 11, 1999, pp. 50–57.

[9]Gossler, A. A., and Marshall, J. S., "Simulation of Normal Vortex-Cylinder Interaction in a Viscous Fluid," *Journal of Fluid Mechanics*, Vol. 431, 2001, pp. 371–405.

J. C. Hermanson
Associate Editor

Two-Step Method for Static Topological Reanalysis

Hua Dong Lian*
Jilin University,
130025 Changchun, People's Republic of China
Xiao Wei Yang†
South China University of Technology,
510640 Guangzhou, People's Republic of China
and
Su Huan Chen‡
Jilin University,
130025 Changchun, People's Republic of China

Nomenclature

$\boldsymbol{K}, \boldsymbol{R}$	=	stiffness matrix and load vectors of the modified structure
$\boldsymbol{K}_F, \boldsymbol{V}_F$	=	stiffness matrix, displacement vector of the transitional structure
$\boldsymbol{K}_R, \boldsymbol{R}_R$	=	stiffness matrix and load vector to determine $\boldsymbol{y}$
$\boldsymbol{K}_0, \boldsymbol{R}_0$	=	stiffness matrix and load vectors of the initial structure
$\boldsymbol{K}_0'$	=	size-expanded stiffness matrix of $\boldsymbol{K}_0$
$\boldsymbol{LDL}^T$	=	factorization of $\boldsymbol{K}_0$
$\boldsymbol{V}, \boldsymbol{V}_0$	=	displacement vectors of the modified and initial structure, respectively
$\boldsymbol{V}_B$	=	basis matrix of displacement vector in the combined approximate procedure
$\boldsymbol{V}_i$	=	ith order perturbation of $\boldsymbol{V}_{n0}$
$\boldsymbol{V}_m$	=	displacement vector of the modified structure for the added m degrees of freedom (DOF)

Received 27 February 2001; revision received 29 August 2001; accepted for publication 4 September 2001.

*Ph.D. Student, Department of Mechanics.
†Associate Professor, Department of Applied Mathematics.
‡Professor, Department of Mechanics; chensh@jlu.edu.cn.

$\boldsymbol{V}_{m0}$ = displacement vector of the transitional system for the added m DOF
$\boldsymbol{V}_n$ = displacement vector of the modified structure for the initial n DOF
$\boldsymbol{V}_{n0}$ = displacement vector of the transitional system for the initial n DOF
$\boldsymbol{y}$ = coefficient vector to be determined in the combined approximate procedure
y_i = coefficients to be determined in the combined approximate procedure
$\Delta\boldsymbol{K}$, $\Delta\boldsymbol{R}$ = change of $\boldsymbol{K}_0$ and $\boldsymbol{R}_0$, respectively, in the reduced-order system
$\Delta\boldsymbol{K}_{mm}$ = submatrix of stiffness of the added joints
$\Delta\boldsymbol{K}_{mn}$ = submatrix of stiffness of the added joints linked to the initial ones
$\Delta\boldsymbol{K}_{nm}$ = submatrix of stiffness of the initial joints linked to the added ones
$\Delta\boldsymbol{K}_{nn}$ = change of the initial stiffness matrix
$\Delta\boldsymbol{K}_0'$ = increment $\boldsymbol{K}$ relative to $\boldsymbol{K}_0'$
$\Delta\boldsymbol{V}_n$, $\Delta\boldsymbol{V}_m$ = increment of $\boldsymbol{V}_{n0}$, $\boldsymbol{V}_{m0}$, respectively

Introduction

STRUCTURAL reanalysis has been the subject of numerous studies in recent years[1–5] because high computational cost involved in repeated designs can be saved. At present, the various topological reanalyses can be classified as follows[6]:

1) The first is deletion of members and joints, where both the design variable vector and the number of degrees of freedom (DOFs) are reduced. When only members are deleted, the value of some design variables becomes zero and can be eliminated from the set of variables, but the analysis model is unchanged.

2) Next is the addition of members and joints, where both the design variable vector and the number of DOFs are increased. If only members are added, then the vector of design variable is expanded, but the number of DOFs is unchanged.

3) The final one is modification in the geometry, where there is no change in the number of variables and in the number of DOFs. In this case only the numerical values of the variables are modified.

Previous studies have developed the methods for the cases of deletion of members and joints, addition of members only, and modifications in the geometry of the structure. Little work has been done for the case in which the number of DOFs is added, and therefore the structural behavior is significantly changed.

Recently, Chen et al.[7] have given a new method for solving the problems in which members and joints are added. In the method the solution process is classified into two steps: establishing a transitional stiffness and matrix making further changes. From Eq. (10) in Ref. 7, it can be seen that the authors do approximation twice; therefore, its accuracy is limited. To improve the accuracy of the method, an effective two-step method will be presented in the Note.

Description of the Problem

Static analysis of the initial structure involves solving a set of simultaneous equations

$$\boldsymbol{K}_0\boldsymbol{V}_0 = \boldsymbol{R}_0 \tag{1}$$

where $\boldsymbol{R}_0$ is assumed to be independent of the design variables. The structural changes will result in a changed stiffness matrix and a changed solution, which satisfy

$$\boldsymbol{K}\boldsymbol{V} = \boldsymbol{R} \tag{2}$$

where $\boldsymbol{K} = (\boldsymbol{K}_0' + \Delta\boldsymbol{K}')$ and

$$\boldsymbol{K}_0' = \begin{bmatrix} \boldsymbol{K}_0 & 0 \\ 0 & 0 \end{bmatrix}, \qquad \Delta\boldsymbol{K}' = \begin{bmatrix} \Delta\boldsymbol{K}_{nn} & \Delta\boldsymbol{K}_{nm} \\ \Delta\boldsymbol{K}_{mn} & \Delta\boldsymbol{K}_{mm} \end{bmatrix} \tag{3}$$

To simplify, the new joints are not loaded, i.e., $\boldsymbol{R}^T = (\boldsymbol{R}_0, 0)$.

It is the problem for given $\boldsymbol{K}_0$ and $\boldsymbol{V}_0$ to find approximate solutions for the modified structure without solving Eq. (2) directly. Basic information we should remember before reanalysis is the $\boldsymbol{LDL}^T$ of $\boldsymbol{K}_0$, which can be obtained easily in the process of many designs.

Reanalysis Method

The reanalysis method can be divided into two steps as follows. First, a transitional equation is given:

$$\boldsymbol{K}_F\boldsymbol{V}_F = \boldsymbol{R} \tag{4}$$

where

$$\boldsymbol{K}_F = \begin{bmatrix} \boldsymbol{K}_0 & 0 \\ 0 & 0 \end{bmatrix} + \begin{bmatrix} 0 & \Delta\boldsymbol{K}_{nm} \\ \Delta\boldsymbol{K}_{mn} & \Delta\boldsymbol{K}_{mm} \end{bmatrix} = \begin{bmatrix} \boldsymbol{K}_0 & \Delta\boldsymbol{K}_{nm} \\ \Delta\boldsymbol{K}_{mn} & \Delta\boldsymbol{K}_{mm} \end{bmatrix} \tag{5}$$

From Eq. (5) it can be seen that some important properties of the original stiffness matrix (symmetry) are preserved in Eq. (4), but positive definiteness is not. Fortunately, no problem arises for the factorization such as $\boldsymbol{LDL}^T$. The $\boldsymbol{LDL}^T$ factorization produces the factors by processing principal diagonal submatrices. It starts with a 1×1 submatrix and then moves through a 2×2 and a 3×3 submatrix, progressively producing and factoring larger leading diagonal submatrices by adding one row and one column, until the factored submatrix is the complete matrix $\boldsymbol{K}_F$. With the $\boldsymbol{LDL}^T$ factorization of Eq. (5), one can obtain the exact values of the modified initial displacement vector from Eq. (4) by forward and backward substitution.

Next, to obtain the solution of the modified structures, let

$$\boldsymbol{V} = (\boldsymbol{V}_n, \boldsymbol{V}_m)^T = (\boldsymbol{V}_{n0} + \Delta\boldsymbol{V}_n, \boldsymbol{V}_{m0} + \Delta\boldsymbol{V}_m)^T \tag{6}$$

It is the key problem to get $(\Delta\boldsymbol{V}_n, \Delta\boldsymbol{V}_m)^T$. Substituting Eq. (6) into Eq. (2) yields

$$\left[\begin{pmatrix} \boldsymbol{K}_0 & \Delta\boldsymbol{K}_{nm} \\ \Delta\boldsymbol{K}_{mn} & \Delta\boldsymbol{K}_{mm} \end{pmatrix} + \begin{pmatrix} \Delta\boldsymbol{K}_{nn} & 0 \\ 0 & 0 \end{pmatrix}\right]\begin{pmatrix} \boldsymbol{V}_{n0} + \Delta\boldsymbol{V}_n \\ \boldsymbol{V}_{m0} + \Delta\boldsymbol{V}_m \end{pmatrix} = \boldsymbol{R} \tag{7}$$

From Eq. (7) one can obtain

$$\begin{pmatrix} \boldsymbol{K}_0 & \Delta\boldsymbol{K}_{nm} \\ \Delta\boldsymbol{K}_{mn} & \Delta\boldsymbol{K}_{mm} \end{pmatrix}\begin{pmatrix} \Delta\boldsymbol{V}_n \\ \Delta\boldsymbol{V}_m \end{pmatrix} + \begin{pmatrix} \Delta\boldsymbol{K}_{nn} & 0 \\ 0 & 0 \end{pmatrix}\begin{pmatrix} \boldsymbol{V}_{n0} + \Delta\boldsymbol{V}_n \\ \boldsymbol{V}_{m0} + \Delta\boldsymbol{V}_m \end{pmatrix} = 0 \tag{8}$$

From Eq. (8) one can obtain the following two equations:

$$\boldsymbol{K}_0\Delta\boldsymbol{V}_n + \Delta\boldsymbol{K}_{nm}\Delta\boldsymbol{V}_m + \Delta\boldsymbol{K}_{nn}(\boldsymbol{V}_{n0} + \Delta\boldsymbol{V}_n) = 0 \tag{9}$$

$$\Delta\boldsymbol{K}_{mn}\Delta\boldsymbol{V}_n + \Delta\boldsymbol{K}_{mm}\Delta\boldsymbol{V}_m = 0 \tag{10}$$

From Eq. (10) one can have

$$\Delta\boldsymbol{V}_m = -\Delta\boldsymbol{K}_{mm}^{-1}\Delta\boldsymbol{K}_{mn}\Delta\boldsymbol{V}_n \tag{11}$$

Substituting Eq. (11) into Eq. (9) yields

$$(\boldsymbol{K}_0 + \Delta\boldsymbol{K})\Delta\boldsymbol{V}_n = \boldsymbol{R}_0 + \Delta\boldsymbol{R} \tag{12}$$

in which

$$\Delta\boldsymbol{K} = \Delta\boldsymbol{K}_{nn} - \Delta\boldsymbol{K}_{nm}\Delta\boldsymbol{K}_{mm}^{-1}\Delta\boldsymbol{K}_{mn}$$

$$\Delta\boldsymbol{R} = -\boldsymbol{R}_0 + \boldsymbol{R}', \qquad \boldsymbol{R}' = -\Delta\boldsymbol{K}_{nn}\boldsymbol{V}_{n0} \tag{13}$$

Using the matrix perturbation theory and combined method presented by Kirsch, one can have

$$\Delta\boldsymbol{V}_n = y_0\boldsymbol{V}_0 + y_1\boldsymbol{V}_1 + y_2\boldsymbol{V}_2 + y_3\boldsymbol{V}_3 = \boldsymbol{V}_B\boldsymbol{y} \tag{14}$$

in which $\boldsymbol{V}_B = [\boldsymbol{V}_0, \boldsymbol{V}_1, \boldsymbol{V}_2, \boldsymbol{V}_3]$, $\boldsymbol{y}^T = \{y_0, y_1, y_2, y_3\}$, and the first three-order perturbation terms resulting from $\Delta\boldsymbol{K}$ can be determined by

$$\boldsymbol{V}_1 = -\boldsymbol{K}_0^{-1}(\Delta\boldsymbol{K}\boldsymbol{V}_0 - \Delta\boldsymbol{R}), \qquad \boldsymbol{V}_2 = -\boldsymbol{K}_0^{-1}\Delta\boldsymbol{K}\boldsymbol{V}_1$$

$$\boldsymbol{V}_3 = -\boldsymbol{K}_0^{-1}\Delta\boldsymbol{K}\boldsymbol{V}_2 \tag{15}$$

Table 1 Comparisons of the displacements at different number of base vectors

Node	Exact (y) (E-3)	2-order (E-3)	Error (E-1)	3-order (E-3)	Error (E-2)	4-order (E-3)	Error (E-3)
11	−0.41210	−0.44993	0.91807	−0.42002	1.9230	−0.41191	0.46135
12	−0.40388	−0.44055	0.90792	−0.41093	1.7446	−0.40350	0.93444
13	−0.63725	−0.67565	0.60267	−0.64493	1.2059	−0.63695	0.46875
14	−0.63811	−0.67664	0.60377	−0.64589	1.2187	−0.63783	0.43739
15	−0.93091	−0.97497	0.47334	−0.93964	0.93802	−0.93085	0.056221
16	−0.93081	−0.97486	0.47325	−0.93954	0.93708	−0.93076	0.058448
17	−1.2716	−1.3246	0.41622	−1.2819	0.80889	−1.2720	0.28506
18	−1.2717	−1.3246	0.41624	−1.2820	0.80897	−1.2720	0.28534
19	−1.6444	−1.7084	0.38923	−1.6566	0.74338	−1.6453	0.54718
20	−1.6440	−1.7080	0.38916	−1.6562	0.74328	−1.6449	0.54643
21	−2.0308	−2.1069	0.37434	−2.0452	0.70530	−2.0323	0.73313
22	−2.0344	−2.1107	0.37489	−2.0488	0.70614	−2.0359	0.73847
25	−0.07949	−0.11312	4.2310	−0.080305	1.0258	−0.079517	0.33826
26	−0.16388	−0.19908	2.1482	−0.16528	0.85578	−0.16376	0.72810
27	−0.27689	−0.31569	1.4014	−0.28315	2.2640	−0.27683	0.21706

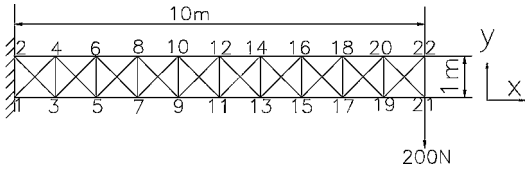

a) Initial design

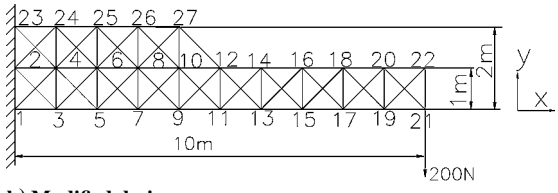

b) Modified design

Fig. 1 Truss structures.

The calculation of the perturbations involves only forward and backward substitution. Thus, the first three-order perturbation terms can be readily calculated. Substituting Eq. (14) into Eq. (12) yields

$$(\boldsymbol{K}_0 + \Delta\boldsymbol{K})\boldsymbol{V}_B\boldsymbol{y} = \boldsymbol{R}_0 + \Delta\boldsymbol{R} \tag{16}$$

Premultiply $\boldsymbol{V}_B^T$ in Eq. (16), and let

$$\boldsymbol{K}_R = \boldsymbol{V}_B^T(\boldsymbol{K}_0 + \Delta\boldsymbol{K})\boldsymbol{V}_B, \qquad \boldsymbol{R}_R = \boldsymbol{V}_B^T\boldsymbol{R}' \tag{17}$$

then one can have

$$\boldsymbol{K}_R\boldsymbol{y} = \boldsymbol{R}_R \tag{18}$$

Thus the coefficient vector $\boldsymbol{y}$ can be determined by solving Eq. (18). Substituting $\boldsymbol{y}$ into Eq. (14), one can obtain a more accurate $\Delta\boldsymbol{V}_n$.

Generally, the first three-order perturbations can give good result in most cases. However, in order to raise the precision more than four base vectors can be adopted, especially for some large changes on the structure. The method can save much labor because we mainly do several backward substitutions and multiplications between matrix and vector, etc., but not to solve Eq. (2) directly, which workload scales with the cube of the dimension of the equation. It is valid even for the multiload case because the number of the load case is usually much smaller than the dimension of the equation.

Numerical Example

Consider an initial truss structure (shown in Fig. 1a) with its parameters: elasticity modulus $E = 2.1 \times 10^{11}$ Pa and cross-section area of each bar $A = 1.2 \times 10^{-4}$ m^2. The modified structure with new added 5 nodes and 17 members is shown in Fig. 1b. The results calculated with a different number of base vectors are shown in Table 1. From Table 1 it can be seen that the proposed method can give good approximations for the displacement of the modified structures. In general, it is enough to give better results to use four base vectors, and the accuracy will be improved with the increase of the number of base vectors. We can also see that the precision is proportional with the size of the displacement, i.e., the larger the exact displacement is, the more accurate the approximate value is, which may be welcome for us because we desire the larger in most cases.

Conclusions

An effective approximate displacement reanalysis method for topological modification has been presented in this Note. In this method the process is divided into two steps. The exact values of the modified initial system are obtained in the first step; the combined approximate method is used in the second one. This procedure is based on the results of initial displacement analysis of the original structures, and little computation effort is involved. This Note is focused on the most challenging case of the addition of joints, in which the number of degrees of freedom is increased. From the numerical examples it has been shown that the proposed method in this Note is effective for displacement reanalysis in topological modifications. The stress obtained by the method may be not as accurate as the displacement because the approximation is based on the displacement. More base vectors should be used if we expect higher precision of stress.

Acknowledgment

This work is supported by the National Natural Science Foundation of China.

References

[1]Chen, S. H., Yang, X. W., and Wu, B. S., "Static Displacement Reanalysis of Structures Using Perturbation and Pade Approximation," *Communications in Numerical Methods in Engineering*, Vol. 16, No. 2, 2000, pp. 75–82.

[2]Chen, S. H., and Yang, X. W., "Extended Kirsch Combined Method for Eigenvalue Reanalysis," *AIAA Journal*, Vol. 38, No. 5, 2000, pp. 927–930.

[3]Rozvany, G. I. N., Bendsoe, M. P., and Kirsch, U., "Layout Optimization of Structures," *Applied Mechanics Reviews*, Vol. 48, No. 2, 1995, pp. 41–118.

[4]Noor, A. K., "Recent Advances and Applications of Reduction Methods," *Applied Mechanics Reviews*, Vol. 47, No. 5, 1994, pp. 125–146.

[5]Kirsch, U., "Improved Stiffness-Based First-Order Approximations for Structural Optimization," *AIAA Journal*, Vol. 33, No. 1, 1995, pp. 143–150.

[6]Kirsch, U., and Liu, S. H., "Structural Reanalysis for General Layout Modifications," *AIAA Journal*, Vol. 35, No. 2, 1997, pp. 382–388.

[7]Chen, S. H., Huang, C., and Liu, Z. S., "Structural Approximate Reanalysis for Topological Modifications of Finite Element Systems," *AIAA Journal*, Vol. 36, No. 9, 1998, pp.1760–1762.

A. Berman
Associate Editor